



Potentiometric studies and molecular docking of quinoline Schiff base and its metal complexes

A.A. El-Bindary^{*a}, A.Z. El-Sonbati^a, M.A. Diab^a, N.A. El-Ghamaz^b,
A.F. Shoair^a, S.G. Nozha^{+,a}

^a Chemistry Department, Faculty of Science, Damietta University, Damietta 34517, Egypt

^b Physics Department, Faculty of Science, Damietta University, Damietta 34517, Egypt

Received 07 Feb 2016, Revised 21 Mar 2016, Accepted 31 Mar 2016

*Corresponding author. E-mail: abindary@yahoo.com; Tel.: +2 01114266996; Fax: +2 0572403868

⁺Abstracted from her Ph.D. Thesis

Abstract

4-{(8-Hydroxyquinolin-7-yl)methyleneamino}-1,2-dihydro-1,5-dimethyl-2-phenylpyrazol-3-one (**HL**) has been synthesized and characterized by different spectroscopic techniques. Molecular docking studies were also performed to illustrate the binding mode of the Schiff base compound **HL**. Docking studies were performed on Protein 3hp5- oxidoreductase receptor of breast cancer. The proton-ligand dissociation constant of the ligand **HL** and metal-ligand stability constants of its complexes with metal ions (Mn^{2+} , Co^{2+} , Ni^{2+} and Cu^{2+}) have been determined potentiometrically in 0.1 M KCl and 20 % (by volume) DMF–water mixture. The stability constants of the formed complexes increases in the order Mn^{2+} , Co^{2+} , Ni^{2+} and Cu^{2+} . The effect of temperature was studied at 298, 308 and 318 K and the corresponding thermodynamic parameters (ΔG , ΔH and ΔS) were derived and discussed. The dissociation process is non-spontaneous, endothermic and entropically unfavorable. The formation of the metal complexes has been found to be spontaneous, endothermic and entropically favorable.

Keywords: Schiff base; Molecular docking; Potentiometric Studies; Quantum calculations.

1. Introduction

Schiff bases have received considerable attention in the literature, because of their interesting properties, various applications and a wide variety of biological activity specially antibacterial and antifungal properties. Important and interesting properties of Schiff bases compounds are directly related to their model character, the presence of an intramolecular hydrogen bond and the conjugative interactions in the molecules [1,2]. Nitrogen heterocyclic compounds have been used widely in the pharmaceutical industry because of their perfect biological activities [3-5]. 8-Hydroxyquinoline is known to be a good chelating reagent and its derivatives have been actively studied [6].

Docking is important in the study of protein ligand interaction properties such as binding energy, geometry complementarity, hydrogen bond donor acceptor, hydrophobicity, electron distribution and polarizability thus it plays a major role in the drug discovery for the identification of suitable molecular scaffold and distinguishing selectivity for the target protein [7]. Quinoline derivatives have also attracted the attention of the chemists because of their presence in many natural products possessing significant biological activities [8,9]. Molecular docking results of 4-chlorophenyl quinoline-2-carboxylate suggested that the compound might exhibit inhibitory activity against glycogen phosphorylase b (GPb) [10].

The proton-ligand dissociation constants of some azo quinoline derivatives and metal-ligand stability constants of their complexes with the metal ions (Mn^{2+} , Co^{2+} , Ni^{2+} and Cu^{2+}) have been determined potentiometrically [11,12]. The azo aldehyde derivatives have one ionizable proton (the enolized hydrogen ion of the hydroxyl

group in the quinoline moiety) while the Azo sulfoxine derivatives have two ionizable protons (the enolized hydrogen ion of the phenolic OH group and the enolized hydrogen ion of the $-\text{SO}_3\text{H}$). The dissociation process is non-spontaneous, endothermic and entropically unfavorable. The formation of the metal complexes has been found to be spontaneous, endothermic and entropically favorable.

The aim of the present work is to study the molecular and electronic structures of the investigated compound **HL** using quantum chemical calculations. Molecular docking was used to predict the binding between Schiff base compound **HL** and the receptor of 3hp5-oxidoreductase receptor of breast cancer. Moreover, the dissociation constant of the Schiff base ligand (**HL**) and the stability constants of its complexes with Mn^{2+} , Co^{2+} , Ni^{2+} and Cu^{2+} at different temperatures. Furthermore, the corresponding thermodynamic functions are evaluated and discussed.

2. Materials and methods

2.1. Measurements

All the compounds and solvents used were purchased from Aldrich and Sigma and used as received without further purification. Elemental microanalyses of the separated ligands for C, H, and N were determined on Automatic Analyzer CHNS Vario ELIII, Germany. The $^1\text{H-NMR}$ spectrum was obtained with a JEOL FX90 Fourier transform spectrometer with DMSO-d_6 as the solvent and TMS as an internal reference. Infrared spectra of the compounds were recorded as KBr discs within the range $4000\text{--}400\text{ cm}^{-1}$ using a Pye Unicam SP 2000 spectrophotometer. The molecular structures of the investigated compounds were optimized by HF method with 3-21G basis set. The molecules were built with the Perkin Elmer ChemBio Draw and optimized using Perkin Elmer ChemBio3D software [13]. Quantum chemical parameters such as the highest occupied molecular orbital energy (E_{HOMO}), the lowest unoccupied molecular orbital energy (E_{LUMO}) and HOMO–LUMO energy gap (ΔE) for the investigated molecules were calculated [14]. In the study simulates the actual docking process in which the ligand–protein pair-wise interaction energies are calculated using Docking Server [15]. The MMFF94 Force field was for used energy minimization of ligand molecule using Docking Server. Gasteiger partial charges were added to the ligand atoms. Non-polar hydrogen atoms were merged, and rotatable bonds were defined. Docking calculations were carried out on 3hb5–OXIDORDUCTASE–Hormone protein model. Essential hydrogen atoms, Kollman united atom type charges, and solvation parameters were added with the aid of AutoDock tools [16]. Affinity (grid) maps of $20\text{X}20\text{X}20\text{ \AA}$ grid points and 375 \AA spacing were generated using the Autogrid program [17]. Auto Dock parameter set- and distance-dependent dielectric functions were used in the calculation of the van der Waals and the electrostatic terms, respectively.

2.2. Synthesis of 4-((8-hydroxyquinolin-7-yl)methyleneamino)-1,2-dihydro-1,5-dimethyl-2-phenyl- pyrazol-3-one (HL)

The ligand was prepared according to the method reported by El-Sonbati and co-workers [18–20]. The ligand (**HL**) has been synthesized by template condensation of 8-hydroxy-7-formylquinoline with 4-amino-1-phenyl-2,3-dimethylpyrazolin-5-one. The mixture was filtered and dried under vacuum to obtain a light yellow powder, MP: $230\text{--}232\text{ }^\circ\text{C}$, yield 75 %. Anal.: Calc. for $\text{C}_{21}\text{H}_{18}\text{N}_4\text{O}_2$ ($M=358$): C, 70.38; H, 5.06; N, 15.63. Found: C, 70.72; H, 4.88; N, 15.87. MS m/z 358 (M^+). The Schiff base ligand (**HL**) is soluble in strong polar solvents such as DMF and DMSO.

1.3. Potentiometric studies

A ligand solution (0.001 M) was prepared by dissolving an accurately weighed amount of the solid in DMF (Analar). Metal ion solutions (0.0001 M) were prepared from Analar metal chlorides in bidistilled water and standardized with EDTA [21]. Solutions of 0.001 M HCl and 1 M KCl were also prepared in bidistilled water. A carbonate-free sodium hydroxide solution in 20 % (by volume) DMF–water mixture was used as titrant and standardized against oxalic acid (Analar).

The apparatus, general conditions and methods of calculation were the same as in previous work [8,22,23]. The following mixtures (i) – (iii) were prepared and titrated potentiometrically at 298 K against standard

0.002 M NaOH in a 20 % (by volume) DMF–water mixture:

i) 5 cm³ 0.001 M HCl + 5 cm³ 1 M KCl + 10 cm³ DMF.

ii) 5 cm³ 0.001 M HCl + 5 cm³ 1 M KCl + 5 cm³ 0.001 M ligand + 5 cm³ DMF.

iii) 5 cm³ 0.001 M HCl + 5 cm³ 1 M KCl + 5 cm³ 0.001 M ligand + 5 cm³ DMF + 10 cm³ 0.0001 M metal chloride.

For each mixture, the volume was made up to 50 cm³ with bidistilled water before the titration. These titrations were repeated for temperatures of 308 and 318 K. All titrations have been carried out between pH 3.0 – 11.0 and under nitrogen atmosphere.

3. Results and discussion

3.1. ¹H and ¹³C NMR spectroscopy

3.1.1. ¹H NMR Spectra

The NMR (¹H and ¹³C) spectra of Schiff base ligand (**HL**) was recorded in DMSO-d₆. The ¹H NMR spectrum of aromatic protons (Ar-H) of **HL** in the quinoline and benzene rings appeared as a multiple range at 6.94-7.91 ppm (Table 1).

Table 1: ¹H NMR spectral data (ppm) in DMSO-d₆ of Schiff base ligand (**HL**).

Assignment	Compound ¹ H NMR δ, ppm (H atoms, peak assignment)
H ₂	8.84
H ₃	7.53
H ₄	8.26
H ₅	7.43
H ₆	7.56
H ₇	7.22
OH	11.08
C-CH ₃	2.38
N-CH ₃	2.51
NH ₂	-
ArH	6.94-7.91
-CH=N-	9.42

The signal at 2.38 and 2.51 ppm are assigned to the methyl [(=C-CH₃ and N-CH₃) groups], and equivalent to three protons each. The coordination of the azomethine (CHN) nitrogen was assigned by the downfield shifting of the -CH=N- proton present originally at 9.42 ppm in the free ligand. **HL** showed a broad peak at 11.08 ppm for OH proton of quinoline ring. The very weak and broad band of hydroxyl proton was most probably resulted from intra-bonding of OH proton with N atoms of azomethine group and quinoline cycle. The weakening and broadening of this type of proton signal might be caused by dimer formation between two hydroxylquinoline groups of two different molecules [24]. The Schiff base ligand (**HL**) prepared may exist in three possible tautomeric forms (A, B and C) as depicted in Fig. 1.

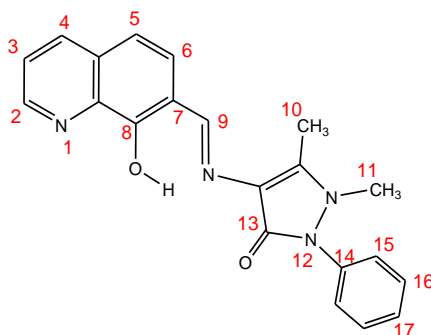
3.1.2. ¹³C NMR spectra

The ¹³C NMR spectra (Table 2) of the Schiff base ligand **HL** was carried out in DMSO-d₆. The singlet peaks at 10.3 and 35.6 ppm are due to the methyl (-CH₃) carbons. The spectrum of the Schiff base ligand, display pyrazolone and quinoline carbons (C=C) in the region 156.5-120.2 ppm, the singlet peak at 160.0 and 160.6 ppm corresponding to the carbonyl carbon and azomethine carbon of Schiff base. In the ¹³C NMR there is no detectable signal for the carbon of carbonyl group (C₈=O) at quinoline ring for the (C) form. Also, the broad

band (C₈-OH signal) was determined from the (A) form of **HL** in the ¹H NMR spectrum. The signal for the N-H proton of **HL** ligand for the carbonyl form was not observed in DMSO-d₆.

Table 2: ¹³C NMR spectral data (ppm) of Schiff base ligand (**HL**).

Assignment	Compound
	¹³ C NMR δ, ppm (C atoms, peak assignment)
C ₂	156.5
C ₃	122.4
C ₄	136.9
C ₅	118.5
C ₆	130.6
C ₇	120.2
C ₈	160.5
C ₉	160.6
C ₁₀	10.3
C ₁₁	35.6
C ₁₃	160.0
C ₁₄	134.3
C ₁₅	124.6
C ₁₆	129.3
C ₁₇	127.3



3.2. IR spectra and mode of coordination

The formation of Schiff base ligand (**HL**) is confirmed by the absence of stretching vibration due to amine (NH₂) moiety of 4-amino-1-phenyl-2,3-dimethylpyrazolin-5-one and instead a strong new band appeared at ~1615 cm⁻¹ corresponding to the azomethine (C=N) group [25,26]. Additionally, IR spectrum of the ligand (**HL**) shows a broad band assigned to phenolic OH group; ν(OH) [19,27,28] and a strong band at 1305 cm⁻¹ assigned to the stretching frequency of the phenolic C-O bond. The bands appearing in the region 1480 and 750 cm⁻¹ were usual modes of phenyl ring vibration [19,27], while a band at 2848 cm⁻¹ for CH₃ stretching vibrations of methyl group [20]. This suggested that amine and carbonyl groups of the starting reagents have been converted into their corresponding Schiff base.

3.3. Geometrical structure

The optimized structure of ligand (**HL**) [tautomeric form (A)] is given in Fig. 2. The selected geometrical structures of the investigated ligand (**HL**) [tautomeric form (A)] were calculated. It was found that the form (A) more stable than other forms. The bond lengths and bond angles for ligand (**HL**) [tautomeric form (A)] listed in Table 3. The C(10)-N(9) bond with length 1.276 Å for ligand (**HL**) [tautomeric form (A)] is a normal imine bond.

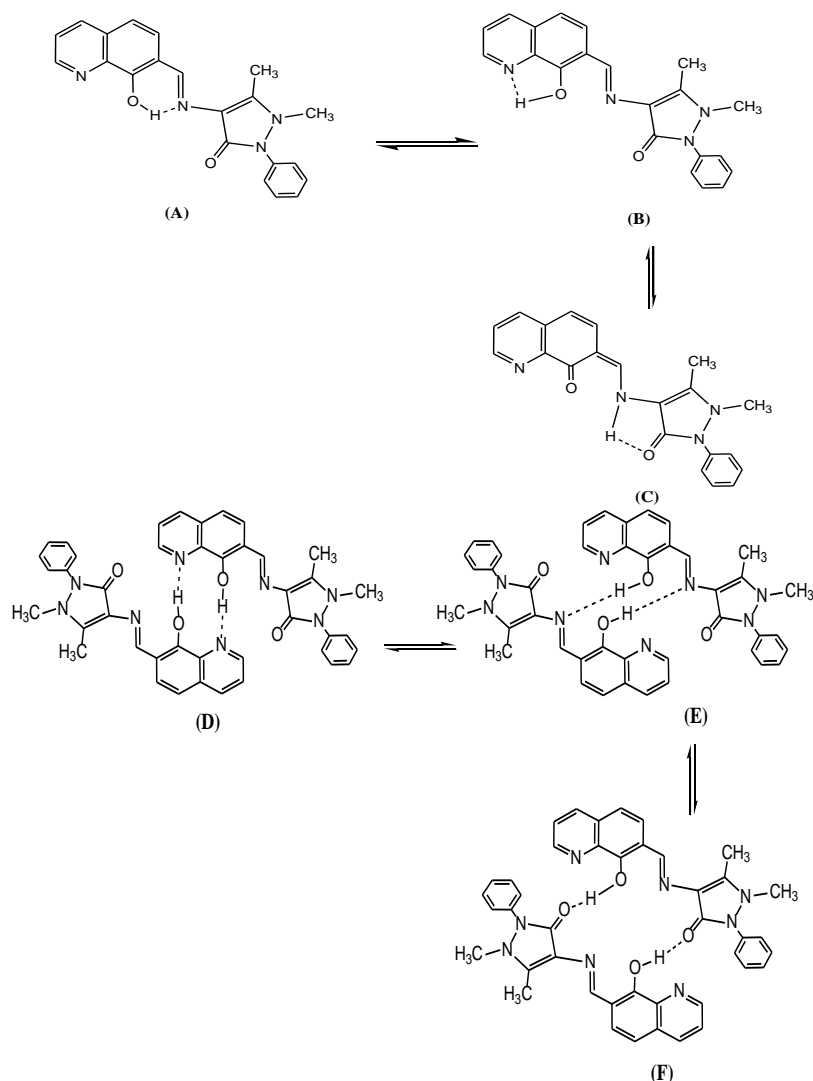


Figure 1: Structure of intramolecular & intermolecular hydrogen bond of Schiff base ligand (**HL**).

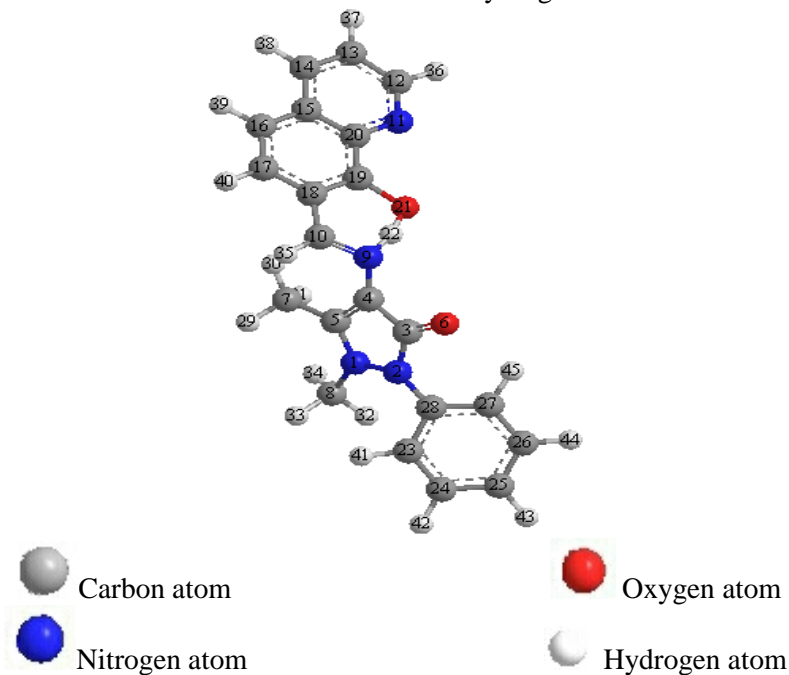


Figure 2: Molecular structure with atomic numbering for Schiff base ligand (**HL**) [tautomeric form (A)].

The HOMO and LUMO are shown in Fig. 3. The HOMO–LUMO energy gap, ΔE , which is an important stability index, is applied to develop theoretical models for explaining the structure and conformation barriers in many molecular systems [29]. The value of ΔE for tautomeric form (**A**) was found to be 0.0381a.u. The calculated quantum chemical parameters are given in Table 4. Additional parameters such as ΔE , absolute electronegativities, χ , chemical potentials, Pi , absolute hardness, η , absolute softness, σ , global electrophilicity, ω , global softness, S , and additional electronic charge, ΔN_{\max} , have been calculated according to the following equations [30,31]:

$$\Delta E = E_{LUMO} - E_{HOMO} \quad (1)$$

$$\chi = \frac{-(E_{HOMO} + E_{LUMO})}{2} \quad (2)$$

$$\eta = \frac{E_{LUMO} - E_{HOMO}}{2} \quad (3)$$

$$\sigma = \frac{1}{\eta} \quad (4)$$

$$Pi = -\chi \quad (5)$$

$$S = \frac{1}{2\eta} \quad (6)$$

$$\omega = \frac{Pi^2}{2\eta} \quad (7)$$

$$\Delta N_{\max} = -\frac{Pi}{\eta} \quad (8)$$

Table 3: The selected geometric parameters for Schiff base ligand (**HL**) [tautomeric form (**A**)].

Bond lengths (Å)		Bond angles (o)		Bond angles (o)	
C(27)-H(45)	1.102	H(44)-C(26)-C(27)	120.118	C(16)-C(15)-C(14)	121.128
C(26)-H(44)	1.103	H(44)-C(26)-C(25)	119.592	H(39)-C(16)-C(17)	118.644
C(25)-H(43)	1.103	C(27)-C(26)-C(25)	120.288	H(39)-C(16)-C(15)	120.868
C(24)-H(42)	1.103	H(43)-C(25)-C(26)	120.51	C(17)-C(16)-C(15)	120.487
C(23)-H(41)	1.102	H(43)-C(25)-C(24)	120.5	O(21)-C(19)-C(20)	124.014
C(17)-H(40)	1.103	C(26)-C(25)-C(24)	118.989	O(21)-C(19)-C(18)	116.934
C(16)-H(39)	1.103	H(42)-C(24)-C(25)	119.766	C(20)-C(19)-C(18)	119.049
C(14)-H(38)	1.103	H(42)-C(24)-C(23)	120.17	H(40)-C(17)-C(18)	120.824
C(13)-H(37)	1.102	C(25)-C(24)-C(23)	120.059	H(40)-C(17)-C(16)	120.061
C(12)-H(36)	1.103	H(45)-C(27)-C(28)	121.851	C(18)-C(17)-C(16)	119.114
C(10)-H(35)	1.104	H(45)-C(27)-C(26)	116.123	C(10)-C(18)-C(19)	113.613
C(8)-H(34)	1.11	C(28)-C(27)-C(26)	121.992	C(10)-C(18)-C(17)	125.018
C(8)-H(33)	1.113	H(41)-C(23)-C(28)	120.899	C(19)-C(18)-C(17)	121.366
C(8)-H(32)	1.112	H(41)-C(23)-C(24)	116.799	N(9)-H(22)-O(21)	167.314
C(7)-H(31)	1.113	C(28)-C(23)-C(24)	122.266	H(35)-C(10)-N(9)	119.084
C(7)-H(30)	1.107	C(23)-C(28)-C(27)	116.394	H(35)-C(10)-C(18)	121.734
C(7)-H(29)	1.113	C(23)-C(28)-N(2)	119.916	N(9)-C(10)-C(18)	119.15
C(23)-C(28)	1.349	C(27)-C(28)-N(2)	123.673	H(31)-C(7)-H(30)	105.545
C(27)-C(28)	1.349	H(34)-C(8)-H(33)	107.904	H(31)-C(7)-H(29)	109.217
C(26)-C(27)	1.343	H(34)-C(8)-H(32)	103.782	H(31)-C(7)-C(5)	110.21
C(25)-C(26)	1.34	H(34)-C(8)-N(1)	113.874	H(30)-C(7)-H(29)	106.125
C(24)-C(25)	1.34	H(33)-C(8)-H(32)	109.808	H(30)-C(7)-C(5)	115.167
C(23)-C(24)	1.342	H(33)-C(8)-N(1)	110.323	H(29)-C(7)-C(5)	110.313
N(1)-C(5)	1.278				

C(4)-C(5)	1.348	H(32)-C(8)-N(1)	110.908	C(5)-N(1)-N(2)	114.216
C(3)-C(4)	1.365	C(3)-N(2)-N(1)	102.731	C(5)-N(1)-C(8)	116.679
N(2)-C(3)	1.274	C(3)-N(2)-C(28)	129.107	N(2)-N(1)-C(8)	128.974
N(1)-N(2)	1.363	N(1)-N(2)-C(28)	123.141	H(22)-N(9)-C(4)	113.299
N(2)-C(28)	1.279	H(37)-C(13)-C(14)	121.214	H(22)-N(9)-C(10)	102.946
H(22)-N(9)	1.038	H(37)-C(13)-C(12)	121.157	C(4)-N(9)-C(10)	118.379
O(21)-H(22)	1	C(14)-C(13)-C(12)	117.629	C(4)-C(5)-C(7)	127.103
C(4)-N(9)	1.272	H(36)-C(12)-C(13)	119.979	C(5)-C(4)-C(3)	106.549
N(9)-C(10)	1.276	H(36)-C(12)-N(11)	116.328	C(5)-C(4)-N(9)	131.394
C(10)-C(18)	1.351	C(13)-C(12)-N(11)	123.692	C(3)-C(4)-N(9)	122.05
C(19)-O(21)	1.378	H(22)-O(21)-C(19)	99.949	C(4)-C(3)-N(2)	111.332
C(15)-C(20)	1.35	C(20)-N(11)-C(12)	119.563	C(4)-C(3)-O(6)	124.081
N(11)-C(20)	1.269	C(15)-C(20)-N(11)	121.827	N(2)-C(3)-O(6)	124.477
C(19)-C(20)	1.348	C(15)-C(20)-C(19)	119.837	Dihedral angles (o)	
C(18)-C(19)	1.351	N(11)-C(20)-C(19)	118.336	C(3)-C(4)-C(5)-N(1)	0.632
C(16)-C(17)	1.341	H(38)-C(14)-C(15)	121.87	C(15)-C(16)-C(17)-C(18)	0.239
C(13)-C(14)	1.34	H(38)-C(14)-C(13)	119.569	C(14)-C(15)-C(16)-C(17)	179.896
N(11)-C(12)	1.265	C(15)-C(14)-C(13)	118.561	C(12)-N(11)-C(20)-C(15)	0.073
N(1)-C(8)	1.486	C(20)-C(15)-C(16)	120.145	C(10)-C(18)-C(19)-C(20)	179.578
C(5)-C(7)	1.51	C(20)-C(15)-C(14)	118.727	C(28)-C(23)-C(24)-C(25)	0.337
C(3)-O(6)	1.215	N(1)-C(5)-C(4)	104.638	C(26)-C(27)-C(28)-N(2)	179.692
		N(1)-C(5)-C(7)	128.255	N(1)-C(5)-C(7)-H(29)	50.502

Table 4: The calculated quantum chemical parameters for Schiff base ligand (**HL**). [tautomeric form (**A**)].

E_{HOMO} (a.u)	E_{LUMO} (a.u)	ΔE (a.u)	χ (a.u)	η (a.u)	σ (a.u) ⁻¹	Pi (a.u)	S (a.u) ⁻¹	ω (a.u)	ΔN_{max}
-0.1378	-0.0998	0.0381	0.1188	0.0190	52.535	-0.1188	26.267	0.371	6.241

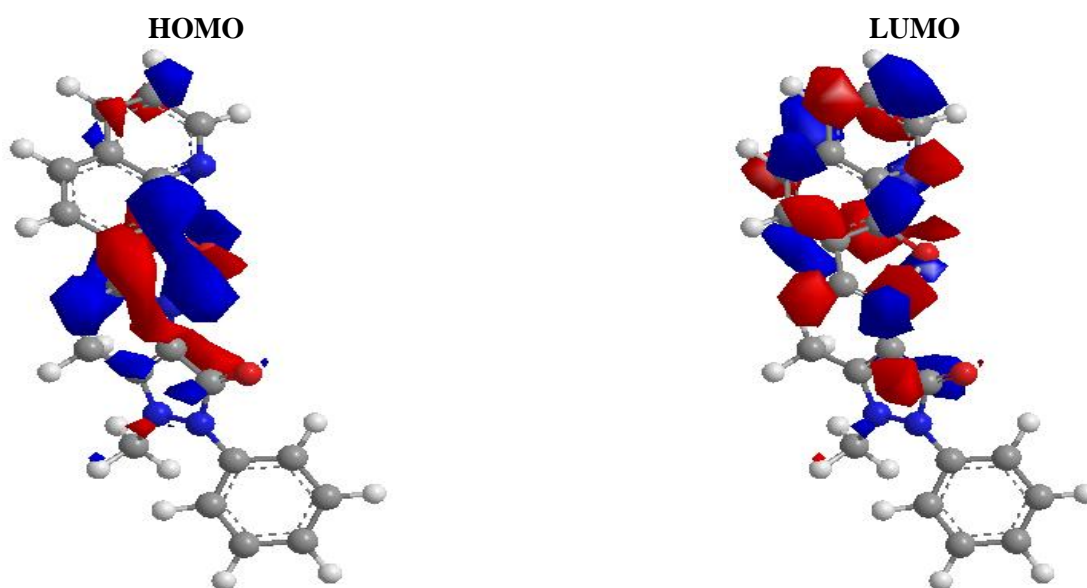


Figure 3: The Highest Occupied Molecular Orbital (HOMO) and the Lowest Unoccupied Molecular Orbital (LUMO) of Schiff base ligand (**HL**) [tautomeric form (**A**)].

3.4. Molecular docking

Cancer can be described as the uncontrolled growth of abnormal cells. Breast cancer is one of the most recurring worldwide diagnosed and deadliest cancers next to lung cancer with a high number of mortality rates among females [32]. At global level, it accounted for more than 1.6 million new cases in 2010. The incidence or prevalence rate of the breast cancer in India is expected to be more than 90,000 in the coming years and over 50,000 women die each year.

Molecular docking is a key tool in computer drug design [33]. The focus of molecular docking is to simulate the molecular recognition process. Molecular docking aims to achieve an optimized conformation for both the protein and drug with relative orientation between them such that the free energy of the overall system is minimized. In this context, we used molecular docking between Schiff base ligand (**HL**) and breast Cancer (3hb5). The results showed a possible arrangement between ligand (**HL**) and receptor (3hb5). On a docking study showing a favorable interaction between ligand (**HL**) and the receptor (3hb5) and the calculated of energy listed in Table 5 and Fig. 4 (A, B) for receptor 3hb5.

Table 5: Energy values obtained in docking calculations of Schiff base ligand (**HL**) with receptor breast cancer mutant 3hb5.

Receptor	Est. free energy of binding (kCal/mol)	Est. inhibition constant (K_i) (μ M)	vdW+ bond+ desolv energy (kCal/mol)	Electrostatic Energy (kCal/mol)	Total Inter-cooled Energy (kCal/mol)	Interact surface
3hb5	-7.46	3.39	-8.68	-0.01	-8.70	926.349

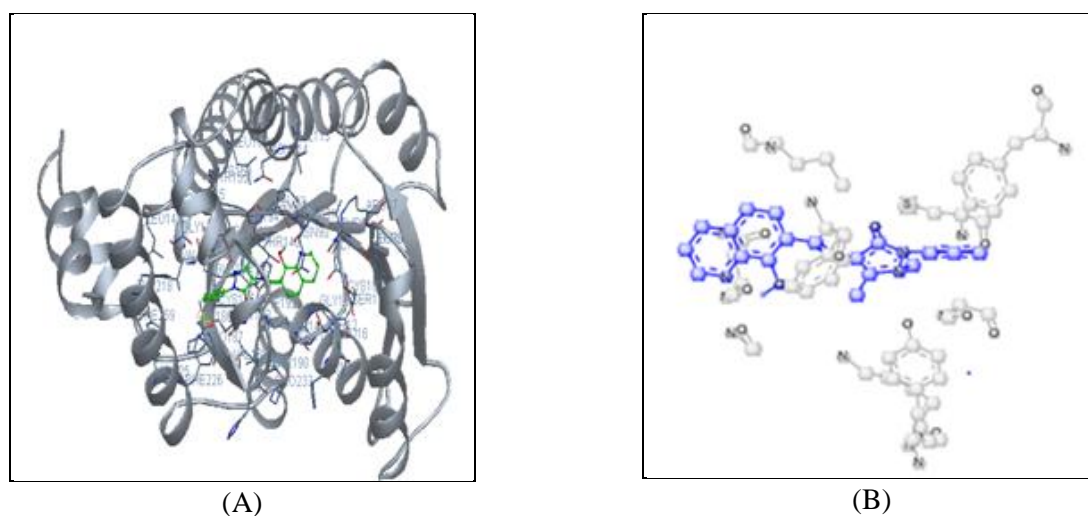


Figure 4: The Schiff base ligand (**HL**) (green in (A) and blue in (B)) in interaction with receptor breast cancer mutant 3hb5. (For interpretation of the references to color in this figure legend, the reader is referred to the web version of this article).

According to our results, HB plot curve indicate that, the ligand (**HL**) binds to the protein with hydrogen bond interactions and decomposed interaction energies in kCal/mole exist of ligand (**HL**) with 3hb5 as shown in Fig. 5 and Table 6. The ligand (**HL**) has a great affinity (pKI) for 3hb5 receptor. The calculated efficiency is favorable, K_i values estimated by AutoDock were compared with experimental K_i values, when available, and the Gibbs free energy is negative. Also, based on this data, we can propose that interaction between the 3hp5 receptor and the ligand (**HL**) is possible. 2D plot curves of docking with ligand (**HL**) are shown in Fig. 6. This interaction could activate apoptosis in cancer cells energy of interactions with ligand (**HL**). Binding energies are most widely used mode of measuring binding affinity of a ligand. Thus, decrease in binding energy due to mutation will increase the binding affinity of the Schiff base ligand towards the receptor. The characteristic

feature of Schiff base ligand represent in presence of several active sites available for hydrogen bonding. This feature gives them the ability to be good binding inhibitors to the protein and will help to produce augmented inhibitory compounds. The results confirm that, the Schiff base ligand derived from 8-hydroxyquinoline-7-aldehyde is efficient inhibitor of 3hb5 – OXID ORDUCTASE breast cancer.

Table 6: Decomposed interaction energies of Schiff base ligand (**HL**) with receptor breast cancer mutant 3hb5.

Receptor	Hydrogen bonds	Polar	Hydrophobic	Other
3hb5	GLY92 (-0.627) TYR155 (-0.4984)		ILE14 (-0.8257) PHE226 (-0.3966) CYS185 (-0.34)	ASN90 (-0.702) LYS159 (-0.283) SER142 (-0.1149)

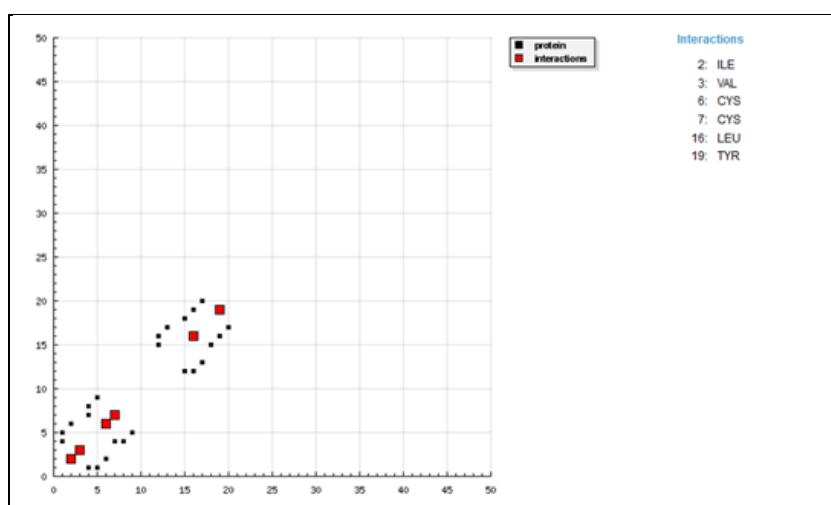


Figure 5: HB plot of interaction between Schiff base ligand (**HL**) with receptor breast cancer mutant 3hb5.

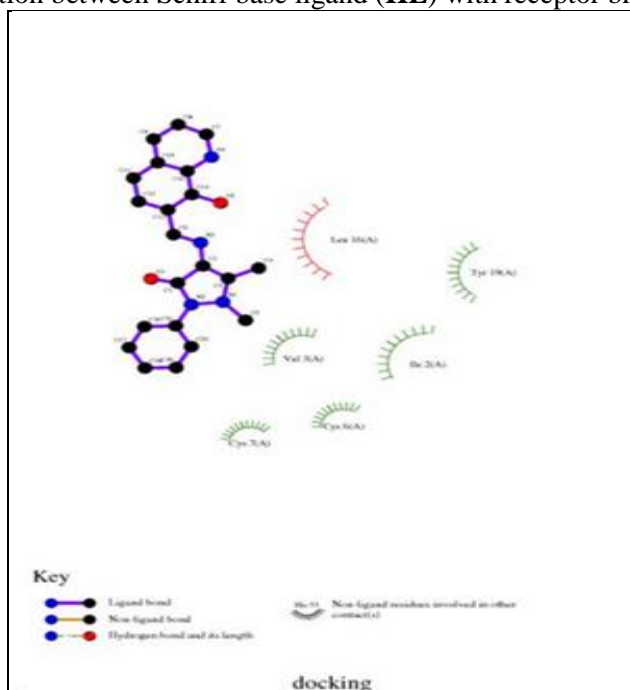


Figure 6: 2D plot of interaction between Schiff base ligand (**HL**) with receptor breast cancer mutant 3hb5.

3.5. Potentiometric measurements

The average number of the protons associated with the Schiff base ligand (**HL**) at different pH values, \bar{n}_A , was calculated from the titration curves of the acid in the absence and presence of **HL**. Applying eq. (9):

$$\bar{n}_A = Y \pm \frac{(V_1 - V_2)(N^\circ + E^\circ)}{(V^\circ - V_1)TC_L^\circ} \quad (9)$$

where Y is the number of available protons in **HL** (Y=1) and V₁ and V₂ are the volumes of alkali required to reach the same pH on the titration curve of hydrochloric acid and reagent, respectively, V^o is the initial volume (50 cm³) of the mixture, TC_L^o is the total concentration of the reagent, N^o is the normality of sodium hydroxide solution and E^o is the initial concentration of the free acid.

Thus, the formation curves (\bar{n}_A vs. pH) for the proton-ligand systems were constructed and found to extend between 0 and 1 in the \bar{n}_A scale (Figure 7). This means that **HL** has one ionizable proton (the enolized hydrogen ion of the hydroxyl group in the quinoline moiety, pK^H). Different computational methods [34] were applied to evaluate the dissociation constant. Three replicate titrations were performed; the average values obtained are listed in Table 7. The completely protonated form of the ligand (**HL**) has one dissociable proton, that dissociates in the measurable pH range.

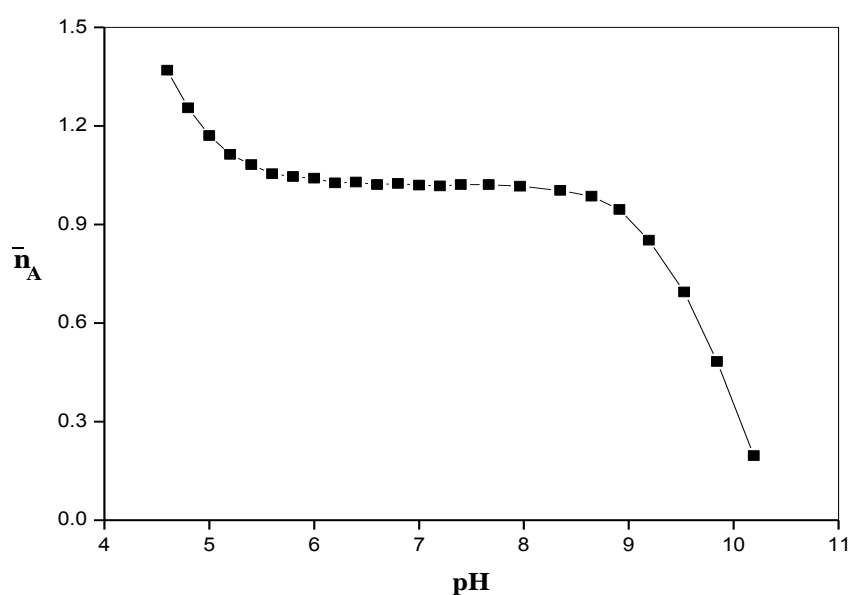


Figure 7: The relation between \bar{n}_A vs. pH for Schiff base ligand (**HL**).

Table 7: Thermodynamic functions for the dissociation of Schiff base ligand (**HL**) in 20 % (by volume) DMF-water mixtures and 0.1 M KCl at different temperatures.

Compound	Temperature	Dissociation	Gibbs energy	Enthalpy Change	Entropy change
	(K)	constant	kJ mol ⁻¹	kJ mol ⁻¹	J mol ⁻¹ K ⁻¹
		pK ^H	ΔG	ΔH	- ΔS
HL	298	9.91	56.54	40.82	52.77
	308	9.68	57.09		52.81
	318	9.46	57.60		52.76

The formation curves for the metal complexes were obtained by plotting the average number of ligand attached per metal ion (\bar{n}) vs. the free ligand exponent (\bar{pL}), according to Irving and Rossotti [35]. The average number of the reagent molecules attached per metal ion, \bar{n} , and free ligand exponent, \bar{pL} , can be calculated using eqs. 10 and 11:

$$\bar{n} = \frac{(V_3 - V_2)(N^\circ + E^\circ)}{(V^\circ - V_2).\bar{n}_A.TC_M^\circ} \quad (10)$$

and

$$pL = \log_{10} \frac{\sum_{n=0}^{n=J} \beta_n^H \left(\frac{1}{[H^+]} \right)^n}{TC_L^o - n.TC_M^o} \cdot \frac{V^o + V_3}{V^o} \quad (11)$$

where TC_M^o is the total concentration of the metal ion present in the solution, β_n^H is the overall proton-reagent stability constant. V_1 , V_2 and V_3 are the volumes of alkali required to reach the same pH on the titration curves of hydrochloric acid, organic ligand and complex, respectively. These curves were analyzed and the successive metal-ligand stability constants were determined using different computational methods [36, 37]. The values of the stability constants ($\log K_1$ and $\log K_2$) are given in Table 8. The following general remarks can be pointed out:

- (i) The maximum value of \bar{n} was ~ 2 indicating the formation of 1:1 and 1:2 (metal: ligand) complexes only [38].
- (ii) The metal ion solution used in the present study was very diluting (2×10^{-5} M), hence there was no possibility of formation of polynuclear complexes [39,40].
- (iii) The metal titration curves were displaced to the right-hand side of the ligand titration curves along the volume axis, indicating proton release upon complex formation of the metal ion with the ligand. The large decrease in pH for the metal titration curves relative to ligand titration curves point to the formation of strong metal complexes [41,42].
- (iv) For the same ligand at constant temperature, the stability of the chelates increases in the order Mn^{2+} , Co^{2+} , Ni^{2+} and Cu^{2+} [43-45]. This order largely reflects that the stability of Cu^{2+} complexes is considerably larger than those of other metals of the 3d series. Under the influence of both the polarizing ability of the metal ion [46] and the ligand field [46] Cu^{2+} will receive some extra stabilization due to tetragonal distortion of octahedral symmetry in its complexes. The greater stability of Cu^{2+} complexes is produced by the well known *Jahn-Teller* effect [47].

Table 8: Stepwise stability constants for complexes of Schiff base ligand (**HL**) in 20 % (by volume) DMF-water mixtures and 0.1 M KCl at different temperatures.

M ⁿ⁺	298 K		308 K		318 K	
	log K ₁	Log K ₂	log K ₁	log K ₂	log K ₁	log K ₂
Mn ²⁺	6.18	4.99	6.31	5.10	6.42	5.23
Co ²⁺	6.33	5.14	6.46	5.25	6.57	5.38
Ni ²⁺	6.47	5.29	6.59	5.40	6.70	5.53
Cu ²⁺	6.63	5.44	6.72	5.56	6.85	5.68

3.6. Effect of temperature

The dissociation constant (pK^H) for **HL**, as well as the stability constants of its complexes with Mn^{2+} , Co^{2+} , Ni^{2+} and Cu^{2+} have been evaluated at 298, 308, and 318 K and are given in Table 9. The enthalpy (ΔH) for the dissociation and complexation process was calculated from the slope of the plot pK^H or $\log K$ vs. $1/T$ using the graphical representation of *Van't Hoff* eqs. 12 and 13:

$$\Delta G = -2.303RT \log K = \Delta H - T\Delta S \quad (12)$$

or

$$\log K = \left(\frac{-\Delta H}{2.303R} \right) \left(\frac{1}{T} \right) + \frac{\Delta S}{2.303R} \quad (13)$$

From the ΔG and ΔH values one can deduce the entropy ΔS using the well known relationships 12 and 14:

$$\Delta S = (\Delta H - \Delta G) / T \quad (14)$$

where $R = 8.314 \text{ J mol}^{-1}\text{K}^{-1}$ is the gas constant, K is the dissociation constant for the ligand or the stability constant of the complex, and T is absolute temperature.

All thermodynamic parameters of the dissociation process of **HL** are recorded in Table 9. From these results the following conclusions can be made:

- (i) The pK^{H} values decrease with increasing temperature, i.e. the acidity of the ligand increases [23].
- (ii) A positive value of ΔH indicates that dissociation is accompanied by absorption of heat and the process is endothermic [48].
- (iii) A positive value of ΔG indicates that the dissociation process is not spontaneous [49].
- (iv) A negative value of ΔS is obtained due to the increased order as a result of the solvation process. All the thermodynamic parameters of the stepwise stability constants of complexes are recorded in Table 9. It is known that the divalent metal ions exist in solution as octahedrally hydrated species [37] and the obtained values of ΔH and ΔS can then be considered as the sum of two contributions: (a) release of H_2O molecules, and (b) metal-ligand bond formation. Examination of these values shows that:
 - (i) The stability constants ($\log K_1$ and $\log K_2$) for **HL** complexes increase with increasing temperature [31].
 - (ii) The negative value of ΔG for the complexation process suggests the spontaneous nature of such processes.
 - (iii) The ΔH values are positive, meaning that these processes are endothermic and favorable at higher temperature.
 - (iv) The ΔS values for the complexes are positive, confirming that the complex formation is entropically favorable [8].

Table 9: Thermodynamic functions for ML and ML_2 complexes of Schiff base ligand (**HL**) in 20 % (by volume) DMF-water mixtures and 0.1 M KCl.

$\text{M}^{\text{n+}}$	T/K	Gibbs energy (kJ mol^{-1})		Enthalpy change (kJ mol^{-1})		Entropy change ($\text{J mol}^{-1} \text{K}^{-1}$)	
		$-\Delta G_1$	$-\Delta G_2$	ΔH_1	ΔH_2	ΔS_1	ΔS_2
Mn^{2+}	298	35.26	28.47	21.78	21.74	191.43	168.52
	308	37.21	30.07			191.55	168.25
	318	39.09	31.84			191.43	168.52
Co^{2+}	298	36.12	29.33	21.87	21.74	194.30	171.39
	308	38.09	30.96			194.42	171.12
	318	40.00	32.75			194.30	171.39
Ni^{2+}	298	36.92	30.18	20.87	21.74	193.91	174.26
	308	38.86	31.84			193.93	173.99
	318	40.79	33.67			193.91	174.26
Cu^{2+}	298	31.04	37.83	20.88	19.91	174.25	193.76
	308	32.78	39.63			174.27	193.32
	318	34.58	41.71			174.44	193.77

Conclusion

The Schiff base ligand of 4-((8-hydroxyquinolin-7-yl)methyleneamino)-1,2-dihydro-1,5-dimethyl-2-phenylpyrazol-3-one (**HL**) has been synthesized and characterized using spectroscopic techniques. The molecular and electronic structures of the investigated compound (**HL**) were studied. Molecular docking confirms that the Schiff base ligand derived from 8-hydroxyquinoline-7-aldehyde is efficient inhibitor of 3hb5-OXID ORDUCTASE breast cancer. The proton-ligand dissociation constant of the ligand (**HL**) and metal-ligand stability constants of their complexes with metal ions (Mn^{2+} , Co^{2+} , Ni^{2+} and Cu^{2+}) have been determined potentiometrically in 0.1 M KCl and 20% (by volume) DMF–water mixture. The corresponding thermodynamic parameters (ΔG , ΔH and ΔS) were derived and discussed. The dissociation process is non-spontaneous, endothermic and entropically unfavorable. The formation of the metal complexes has been found to be spontaneous, endothermic and entropically favorable.

References

1. Dziembowska T., *Pol. J. Chem.* 72 (1998) 193–209.
2. Hadjoudis E., Kerr H., Bouas-Laurent H. (Eds.), *Studies in Organic Chemistry, Photochromism*, Elsevier, Amsterdam, vol. 40, 1990 (Chapter 17).
3. Barraja P., Diana P., Montalbano A., Dattolo G., Cirrincione G., Viola G., Vedaldi D., Acqua F.D., *Bioorg. Med. Chem.* 14 (2006) 8712–8728.
4. Oeveren A.V., Motamedi M., Martinborough E., Zhao S., Xing Y.S., West S., Chang W., Kallem A., Marshchke K.B., Lopez F.J., Andres N., Zhi L., *Bioorg. Med. Chem.* 17 (2007) 1527–1531.
5. Kuethe J.T., Wong A., Qu C.X., Smithrovich J., Davies I.W., Hughes D.L., *J. Org. Chem.* 70 (2005) 2555–2567.
6. Zhang X.X., Bordunov A.V., Bradshaw J.S., Dalley N.K., Izatt R.M., *J. Am. Chem. Soc.* 117 (1995) 11507–11511.
7. El-Sonbati A.Z., Diab M.A., El-Bindary A.A., Mohamed G.G., Morgan, Sh.M., Abou-Dobara, Nozha S.G., *J. Mol. Liq.* 215 (2016) 423–442.
8. Pandey V.K., Tusi S., Misra R., Shukla R., *Indian J. Chem. B*, 49 (2010) 107–111.
9. El-Sonbati A.Z., Abou-Dobara M.I., Diab M.A., El-Bindary A.A., Nozha S.G., *Res. Chem. Intermed.* 42 (2016) 1–33.
10. Fazal E., Panicker C.Y., Varghese H.T., Nagarajan S., Sudha B.S., War J.A., Srivastava S.K., Harikumar B., Anto P.L., *Spectrochim. Acta A* 145 (2015) 260–269.
11. Shoair A.F., El-Bindary A.A., El-Sonbati A.Z., Beshry N.M., *J. Mol. Liq.* 215 (2016) 740–748.
12. El-Bindary A.A., El-Sonbati A.Z., Diab M.A., Ghoneim M.M., Serag L.S., *J. Mol. Liq.* 216 (2016) 318–329.
13. El-Sonbati A.Z., Diab M.A., El-Bindary A.A., Eldesoky A.M., Morgan Sh.M., *Spectrochim. Acta A* 135 (2015) 774–791.
14. El-Ghamaz N.A., El-Sonbati A.Z., Diab M.A., El-Bindary A.A., Awad M.K., Morgan Sh.M., *Mater. Sci. Semicond. Process* 19 (2014) 150–162.
15. Bikadi Z., Hazai E., *J. Chem. Inf.* 11 (2009) 1–15.
16. Halgren T.A., *J. Computat. Chem.* 17 (1998) 490–519.
17. Morris G.M., Goodsell D.S., *J. Comput. Chem.* 19 (1998) 1639–1662.
18. El-Ghamaz N.A., El-Sonbati A.Z., Diab M.A., El-Bindary A.A., Seyam H.A., *Solid State Sci.* 19 (2013) 19–26.
19. El-Sonbati A.Z., Diab M.A., El-Bindary A.A., Abd El-Kader M.K., *Spectrochim. Acta A* 99 (2012) 211–217.
20. El-Ghamaz N.A., Diab M.A., El-Bindary A.A., El-Sonbati A.Z., Seyam H.A., *J. Mater. Sci. Semicond. Proc.* 27 (2014) 521–531.
21. Jeffery G.H., Bassett J., Mendham J., Deney R.C., *Vogel's Text book of Quantitative Chemical Analysis*, 5th Edition. Longman, London (1989).
22. Mubarak A.T., Al-Shihri A.S., Nassef H.M., El-Bindary A.A., *J. Chem. Eng. Data* 55 (2010) 5539–5542.
23. Mubarak A.T., El-Bindary A.A., *J. Chem. Eng. Data* 55 (2010) 5543–5546.
24. Diab M.A., El-Bindary A.A., El-Sonbati A.Z., Salem O.L., *J. Mol. Struct.* 1018 (2012) 176–184.
25. Bassett J., Denney R.C., Jeffery G.H., Mendham J., *Vogel's Textbook of Quantitative Inorganic Analysis*, fourth ed., Longmans, London, 1978.
26. El-Ghamaz N.A., El-Bindary A.A., Diab M.A., El-Sonbati A.Z., Nozha S.G., *Res. Chem. Intermed.* 42 (2016) 2501–2523.
27. El-Sonbati A.Z., Diab M.A., El-Bindary A.A., Abou-Dobara M.I., Seyam H.A., *Spectrochim. Acta A* 104 (2013) 213–221.
28. El-Sonbati A.Z., Diab M.A., El-Bindary A.A., Morgan Sh.M., *Inorg. Chim. Acta* 404 (2013) 175–187.

29. Feng Y., Chen S., Guo W., Zhang Y., Liu G., *J. Electroanal. Chem.* 602 (2007) 115-122.
30. El-Sonbati A.Z., Diab M.A., El-Bindary A.A., Morgan Sh.M., *Spectrochim. Acta. A* 127 (2014) 310-328.
31. El-Bindary A.A., El-Sonbati A.Z., Diab M.A., Morgan Sh.M., *J. Mol. Liq.* 201 (2015) 36-42.
32. Benson J.R., Jatoi I., *Future Oncol.* 8 (2012) 697-702.
33. Beteringhe A., Racuciu C., Balan C., Stoican E., Patron L., *Adv. Mater. Res.* 787 (2013) 236-240.
34. Irving H., Rossotti H. S. , *J. Chem. Soc.* (1954) 2904-2910.
35. Irving H., Rossotti H. S. , *J. Chem. Soc.* (1953) 3397-3405.
36. Rossotti F.J.C., Rossotti H.S., *Acta Chem. Scand.* 9 (1955) 1166-1176.
37. Beck M.T., Nagybal I. , *Chemistry of Complex Equilibrium*, Wiley, New York (1990).
38. Khalil M. M., Radalla A. M. , Mohamed A.G. , *J. Chem. Eng. Data* 54 (2009) 3261-3272.
39. Sanyal P., Sengupta G.P. , *J. Ind. Chem. Soc.* 67 (1990) 342-344.
40. Sridhar S., Kulanthaipandi P., Thillaiarasu P., Thanikachalam V., Manikandan G., *J. Chem.* 4 (2009) 133-140.
41. Athawale V.D., Lele V. , *J. Chem. Eng. Data* 41 (1996) 1015-1019.
42. Athawale V.D., Nerkar S.S. , *Monatsh. Chem.* 13 (2000) 267-276.
43. Ibañez G.A., Escandar G. M. , *Polyhedron* 17 (1998)4433-4441.
44. Malik W.U., Tuli G.D., Madan R.D., *Selected Topics in Inorganic Chemistry*, 3rd Edition. Chand, S. & Company LTD, New Delhi (1984).
45. Mohamed G.G., Omar M.M., Ibrahim A., *Eur. J. Med. Chem.* 44 (2009) 4801-4812.
46. Harlly F.R., Burgess R.M., Alcock R.M., *Solution Equilibria*, Ellis Harwood, Chichester (1980) p.257.
47. Orgel L.E., *An Introduction to Transition Metal Chemistry Ligand Field Theory*, Methuen, London (1966) p. 55.
48. Bhesaniya K.D., Baluja S., *J. Mol. Liq.* 190 (2014) 190-195.
49. Bebot-Bringaud A., Dange C., Fauconnier N., Gerard C., *J. Inorg. Biochem.* 75 (1999) 71-78.

(2016) ; <http://www.jmaterenvironsci.com>